The strange contribution to a_μ with physical quark masses using Möbius domain wall fermions

Matt Spraggs[*a], **Peter Boyle**[b], **Luigi Del Debbio**[b], **Andreas Jüttner**[a], **Christoph Lehner**[c], **Kim Maltman**[d,e], **Marina Marinkovic**[f], **Antonin Portelli**[a,c]

[a] *School of Physics and Astronomy, University of Southampton, Southampton SO17 1BJ, UK*
[b] *SUPA, School of Physics, The University of Edinburgh, Edinburgh EH9 3JZ, UK*
[c] *Physics Department, Brookhaven National Laboratory, Upton, NY 11973, US*
[d] *Department of Physics and Astronomy, York University, Toronto, Ontario, M3J 1P3, Canada*
[e] *CSSM, University of Adelaide, Adelaide, SA 5005, Australia*
[f] *CERN, Physics Department, 1211 Geneva 23, Switzerland*
Email: ms10g12@soton.ac.uk

We present preliminary results for the strange leading-order hadronic contribution to the anomalous magnetic moment of the muon using RBC/UKQCD physical point domain wall fermions ensembles. We discuss various analysis strategies in order to constrain the systematic uncertainty in the final result.

The 33rd International Symposium on Lattice Field Theory,
14-18 July, 2015
Kobe International Conference Center, Kobe, Japan

---

[*]Speaker.

Parameter	48I	64I
$L^3 \times T \times L_s$	$48^3 \times 96 \times 24$	$64^3 \times 128 \times 12$
am_l	0.00078	0.000678
am_s	0.0362	0.02661
a^{-1} / GeV	1.730(4)	2.359(7)
L / fm	5.476(12)	5.354(16)
m_π / MeV	139.2(4)	139.2(5)
m_K / MeV	499.0(12)	507.6(16)
$m_\pi L$	3.863(6)	3.778(8)

Table 1: Ensembles used in this study [7].

1. Introduction

The anomalous magnetic moment of the muon, a_μ, is one of the most accurately determined quantities in particle physics, with an accuracy of the order of one part per million [1]. There is currently a 3σ to 4σ tension between the experimental and theoretical determinations of this quantity. The new muon $g-2$ experiment at Fermilab is expected to reduce the uncertainty from experiment by a factor of four, making a reduction in the theoretical error desirable. The leading-order (LO) hadronic contribution is the main source of this uncertainty. In addition, current estimates of this value are computed using a $\sigma\left(e^+e^- \to \text{hadrons}\right)$ data [2, 3], making a first-principles computation desirable. Here we present the computation of the connected strange contribution to this quantity. We use a variety of analysis techniques in order to test both the techniques and their effect on the final value of a_μ^s.

The LO strange hadronic contribution, a_μ^s, can be computed as follows [4]:

$$a_\mu^s = \left(\frac{\alpha}{\pi}\right)^2 \int_0^\infty \mathrm{d}Q^2 \hat{\Pi}\left(Q^2\right) f\left(Q^2\right), \tag{1.1}$$

where α is the QED coupling, $\hat{\Pi}(Q^2) = 4\pi^2 \left(\Pi^s(Q^2) - \Pi^s(0)\right)$ is the infra-red subtracted hadronic vacuum polarization (HVP) scalar function and f is the integration kernel derived in perturbation theory, with a singularity at $Q^2 = 0$. The resulting integrand is highly peaked near $Q^2 \approx m_\mu^2/4$, meaning that the final value of a_μ is highly sensitive to variations in the values of $\hat{\Pi}(Q^2)$.

Our analysis can be broadly divided into two strategies. The first makes use of the hybrid method outlined in [5]. The second uses continuous momenta in the lattice Fourier transform to compute the scalar HVP function directly at arbitrary momentum [6].

2. Simulation Details

Simulations have been performed on the two 2+1 flavour domain wall fermion (DWF) ensembles with near-physical pion masses described in [7]. For convenience we summarize the properties of these ensembles in Table 1.

We compute the lattice vacuum polarisation, $C_{\mu\nu}$, using $\mathbb{Z}_2$ wall sources and Möbius domain wall fermions, with a local vector current at the source and the DWF conserved vector current at the sink, i.e.:

$$C_{\mu\nu}(x) = \frac{Z_V}{9} \left\langle \mathscr{V}_\mu(x) V_\nu(0) \right\rangle, \tag{2.1}$$

where Z_V is the vector renormalization constant, a is the lattice spacing, V_v is the local vector current and we define the conserved Möbius DWF vector current $\mathcal{V}_\mu(x)$ as described in [7].

To account for a small mistuning in the strange quark mass on each ensemble, we performed a set of partially quenched measurements using the physical value of the strange quark mass. These were performed in addition to the unitary measurements [7].

3. Analysis

We implemented a variety of analysis strategies in order to ascertain the dependence of a_μ on the analysis technique.

3.1 HVP Computation

We can compute the HVP tensor in momentum space by performing a Fourier transform of the position space HVP correlator, i.e.:

$$\Pi_{\mu v}(Q) = \sum_x e^{-iQ \cdot x} C_{\mu v}(x) - \sum_x C_{\mu v}(x), \tag{3.1}$$

where the second summation effectively subtracts the zero-mode [8]. In the infinite volume limit this term is zero, and subtracting it greatly reduces the noise in the low-Q^2 region. For the lowest momentum value of $\Pi(\hat{Q}^2)$ the improvement in the statistical error is approximately a factor of five.

We then perform a tensor decomposition of the HVP tensor, so that it may be related to the scalar HVP function as follows:

$$\Pi_{\mu v}(\hat{Q}) = (\delta_{\mu v}\hat{Q}^2 - \hat{Q}_\mu \hat{Q}_v)\Pi(\hat{Q}^2) + \cdots, \tag{3.2}$$

where the ellipis denotes contributions from Lorentz symmetry breaking, discretisation and finite volume effects and $\hat{Q} = 2\sin(Q/2)$ is the momentum of the intermediate photon. We remove a potential source of lattice cut-off effects by considering only the diagonal component of the HVP tensor where $\hat{Q}_\mu = 0$ [9].

3.2 Hybrid Method

We used the hybrid method as described in [5]. This method consists of partitioning the integrand in (1.1) into three non-overlapping adjacent regions using cuts at low- and high-Q^2. The integrand is then computed for the three regions in different ways. The low-Q^2 region is integrated by modelling $\Pi(Q^2)$ to extrapolate to $\Pi(0)$, which is subtracted to compute $\hat{\Pi}(Q^2)$. This result is then combined with the kernel $f(Q^2)$ to produce the integrand of interest, which is then integrated numerically. The mid-Q^2 region is integrated directly by multiplying the lattice data by $f(Q^2)$ before using the trapezium method. Finally, the high-Q^2 region is integrated by using the result from perturbation theory [10, 5]. Restricting the use of an HVP parameterisation to the low-Q^2 region allows us to minimise systematic effects [5].

We use two classes of parameterisations for the low-Q^2 region when performing the integral in Equation (1.1): Padé approximants and conformal polynomials. The Padé approximants are written as follows [11]:

$$R_{mn}(\hat{Q}^2) = \Pi_0 + \hat{Q}^2\left(\sum_{i=0}^{m-1}\frac{a_i^2}{b_i^2 + \hat{Q}^2} + \delta_{mn}c^2\right), \; n = m, m+1, \tag{3.3}$$

where a_i, b_i, Π_0 and possibly c are parameters to be determined.

The conformal polynomials are written as follows [5]:

$$P_n^E\left(\hat{Q}^2\right) = \Pi_0 + \sum_{i=1}^{n} p_i w^i, \; w = \frac{1 - \sqrt{1+z}}{1 + \sqrt{1+z}}, \; z = \frac{\hat{Q}^2}{E^2}, \tag{3.4}$$

where p_i and Π_0 are parameters to be determined. The parameter E is the two-particle mass threshold.

We use two techniques for constraining the low-Q^2 models: χ^2 minimisation and continuous time moments [12]. The χ^2 minimization involves a fit where the covariance matrix is approximated by its diagonal, i.e. the fit is uncorrelated. This technique lends weight to points in the computed HVP with a smaller statistical error at larger values of Q^2.

The moments method defines a relationship between the HVP scalar function and the lattice space-averaged current-current correlator, $C_{\mu\mu}(t)$.

$$\sum_t e^{-iQ_0 t} C_{\mu\mu}(t) = \hat{Q}_0^2 \Pi\left(\hat{Q}_0^2\right) \tag{3.5}$$

Taking the nth derivate with respect to $\hat{Q}_0$ at $\hat{Q}_0 = 0$ allows us to write

$$(-1)^n \sum_t t^{2n} C_{\mu\mu}(t) = \left. \frac{\partial^{2n}}{\partial Q_0^{2n}} \left(\hat{Q}_0^2 \Pi\left(\hat{Q}_0^2\right)\right) \right|_{Q_0 = 0} \tag{3.6}$$

We then insert one of the above analytical ansätze for the HVP scalar function, setting up a system of equations that can be solved to determine the model parameters.

The moments method uses continuous derivatives, meaning an infinite volume is assumed. When performing the moments method, we use a model that is a function of $\hat{Q}^2$. However, within the moments method, derivatives are taken with respect to Q_0 and not $\hat{Q}_0$. Within the determination of the model parameters, the low-Q^2 cut is not used as an input for this technique, so the resulting parameters do not depend on the low cut used in the hybrid method [12].

3.3 Continuous Momenta

One alternative to the hybrid method is to compute the HVP directly at an arbitrary momentum by performing the Fourier transform at said momentum [6]. Whereas before we used $Q_0 = \frac{2\pi}{T} n_0$ with $n_0 \in \mathbb{Z}$, $-T/2 \leq n_0 < T/2$, we now let n_0 lie anywhere on the half-closed interval $[-T/2, T/2)$. This allows for the computation of a_μ^s without using a parameterisation of the HVP.

Because we are computing the HVP tensor for momenta that are non-Fourier modes on the lattice, there may be some finite volume errors associated with this method. However, it can be shown that these are exponentially suppressed by the lattice volume [6]. Using this technique, we compute the HVP at arbitrary momenta up to some high cut, after which the perturbative result is used.

4. Results

We used nine different parameterisations of the HVP when performing the hybrid method: $P_2^{0.5\text{GeV}}$, $P_3^{0.5\text{GeV}}$, $P_4^{0.5\text{GeV}}$, $P_2^{0.6\text{GeV}}$, $P_3^{0.6\text{GeV}}$, $P_4^{0.6\text{GeV}}$, $R_{0,1}$, $R_{1,1}$ and $R_{1,2}$. We scan three low cuts and three high cuts: 0.5GeV^2, 0.7GeV^2 and 0.9GeV^2, and 4.5GeV^2, 5.0GeV^2 and 5.5GeV^2. We used

the same high cuts when computing a_μ^s using continuous momenta, where we used a step size of 0.005 for n_t.

Figure 1 illustrates an example extrapolation to the continuum and the physical strange quark mass. We perform a two-dimensional linear fit in a^2 and the relative deviation of the strange mass from the physical value. We do this because domain wall fermions are $\mathcal{O}(a)$ improved, and in the latter case we assume a linear dependence of a_μ^s on the strange quark mass. In this case we used the $R_{0,1}$ parameterisation, which was constrained using an uncorrelated χ^2 minimisation. The low cut in this case was 0.5GeV^2 and the high cut was 4.5GeV^2. The effect of the strange quark mistuning is clearly visible, with the final value of a_μ^s shifting from approximatley 50×10^{-10} to 53.0×10^{-10}.
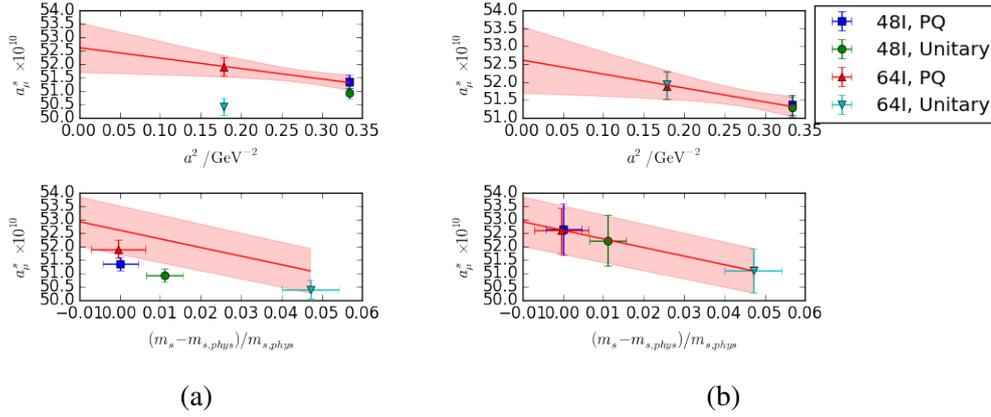

Figure 1: Continuum and strange quark mass extrapolations. In the right-hand set of plots we have subtracted the effects from the strange quark mass (top) and lattice spacing (bottom).

Figure 2 illustrates the variation of a_μ^s as the low cut in the hybrid method is varied. All the computed values of a_μ^s agree within statistics, and most of the values are in strong agreement with one another. Furthermore, our results agree with those of HPQCD [12] and ETMC [13] to within statistics. The models with the fewest parameters, i.e. $P_2^{0.5\text{GeV}}$, $P_2^{0.6\text{GeV}}$ and $R_{0,1}$, deviate slightly from 53.0×10^{-10}. This is more apparent in the case where the models are constrained with χ^2 fits. This is likely a result of the fit favouring data at larger Q^2, where the statistical error is smaller, whilst the moments use an expansion around $Q^2 = 0$, favouring data around this point.

Figure 3 demonstrates the various values of a_μ computed in this analysis. Good agreement is found between all values of a_μ^s. This suggests that the systematic error resulting from the various analysis techniques is small.

5. Summary

We have computed the strange contribution to the anomalous magnetic moment of the muon using domain wall fermions with physical quark masses. We used a variety of analysis techniques, in particular the hybrid method proposed in [5] and continuous momenta [6]. Our final values of a_μ^s show good agreement with each other, suggesting that the systematic error from the choice of analysis technique is small. Furthermore, we find good agreement with the work of HPQCD [12] and ETMC [13].

We are now in the process of finalising the analysis of possible sources of systematic error, particularly finite volume effects. We are simultaneously extending our analysis to the connected
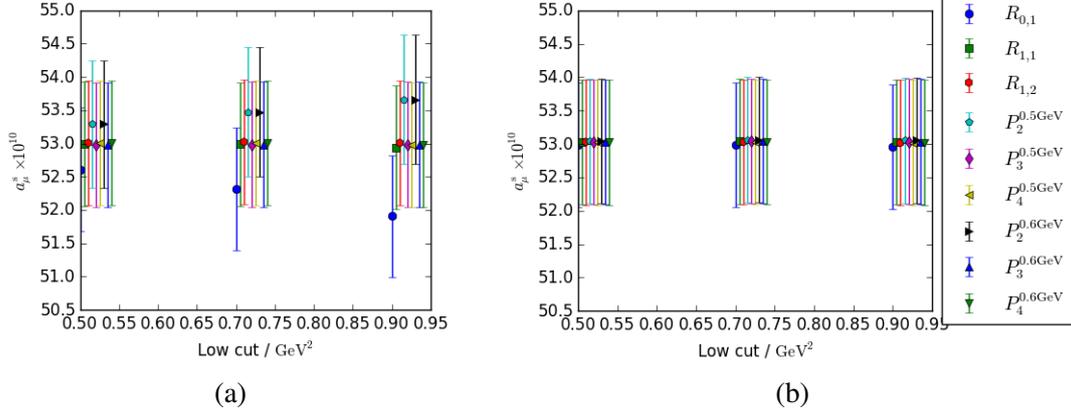
Figure 2: Computed values of a_μ^s against various low cuts for fits (left) and moments (right).
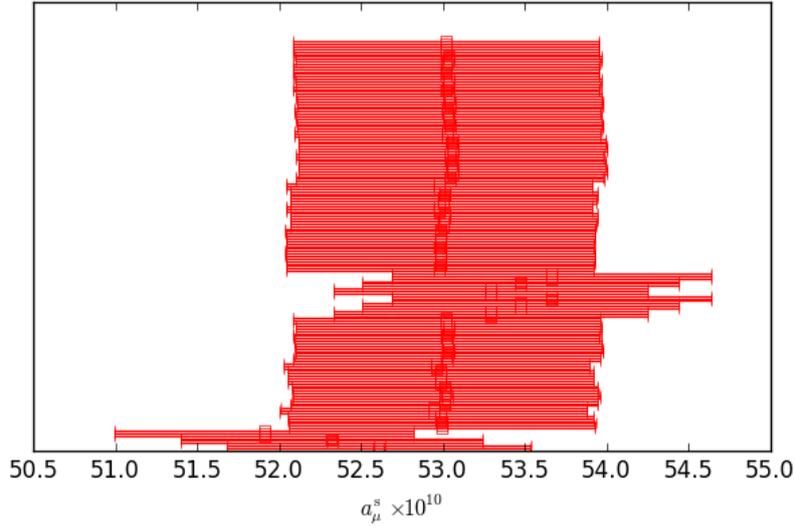

Figure 3: Errorbar plot illustrating the various values of a_μ computed in this analysis.

light contribution contribution to a_μ. In the future we plan to account for the effect of disconnected diagrams.

6. Acknowledgements

References

[1] F. Jegerlehner and A. Nyffeler. *The Muon g-2. Phys. Rept.* **477** pp. 1–110 (2009). doi:10.1016/j.physrep.2009.04.003

[2] M. Davier, A. Hoecker, B. Malaescu and Z. Zhang. *Reevaluation of the Hadronic Contributions to the Muon g-2 and to alpha(MZ). Eur. Phys. J.* **C71** p. 1515 (2011). [Erratum: Eur. Phys. J.C72,1874(2012)], doi:10.1140/epjc/s10052-010-1515-z

[3] K. Hagiwara *et al.* $(g-2)_\mu$ *and alpha*(M_Z^2) *re-evaluated using new precise data. J. Phys.* **G38** p. 085003 (2011). doi:10.1088/0954-3899/38/8/085003

[4] T. Blum. *Lattice calculation of the lowest order hadronic contribution to the muon anomalous magnetic moment. Phys. Rev. Lett.* **91** p. 052001 (2003). doi:10.1103/PhysRevLett.91.052001

[5] M. Golterman, K. Maltman and S. Peris. *New strategy for the lattice evaluation of the leading order hadronic contribution to* $(g-2)_\mu$. *Phys.Rev.* **D90**(7) p. 074508 (2014). doi:10.1103/PhysRevD.90.074508

[6] L. Del Debbio and A. Portelli (to appear)

[7] T. Blum *et al.* (RBC, UKQCD). *Domain wall QCD with physical quark masses* (2014). arXiv:1411.7017

[8] D. Bernecker and H. B. Meyer. *Vector Correlators in Lattice QCD: Methods and applications. Eur. Phys. J.* **A47** p. 148 (2011). doi:10.1140/epja/i2011-11148-6

[9] P. Boyle, L. Del Debbio, E. Kerrane and J. Zanotti. *Lattice Determination of the Hadronic Contribution to the Muon g − 2 using Dynamical Domain Wall Fermions. Phys. Rev.* **D85** p. 074504 (2012). doi:10.1103/PhysRevD.85.074504

[10] K. G. Chetyrkin, J. H. Kuhn and M. Steinhauser. *Three loop polarization function and O (alpha-s**2) corrections to the production of heavy quarks. Nucl. Phys.* **B482** pp. 213–240 (1996). doi:10.1016/S0550-3213(96)00534-2

[11] C. Aubin, T. Blum, M. Golterman and S. Peris. *Model-independent parametrization of the hadronic vacuum polarization and g-2 for the muon on the lattice. Phys. Rev.* **D86** p. 054509 (2012). doi:10.1103/PhysRevD.86.054509

[12] B. Chakraborty *et al.* (HPQCD). *Strange and charm quark contributions to the anomalous magnetic moment of the muon. Phys. Rev.* **D89**(11) p. 114501 (2014). doi:10.1103/PhysRevD.89.114501

[13] X. Feng *et al. Computing the hadronic vacuum polarization function by analytic continuation. Phys. Rev.* **D88** p. 034505 (2013). doi:10.1103/PhysRevD.88.034505